Distance–time parameters designed for mine seismicity

Laura Camball [a,*], David Landry [b], Navita Ramdass [b], Ana Leite [b]

[a] *Mine Seismix, Canada*

[b] *Coleman Mine, Vale Base Metals, Canada*

Abstract

In deep and high stress mining environments, blasting routinely induces and triggers dynamic rock mass failure. This complex interdependence is challenging to understand, particularly using traditional seismic source parameters and techniques adapted from earthquake seismology. Distance time (DT) parameters are mining specific, designed to quantitatively differentiate between Type A (induced) and Type B (triggered) seismic events in mines. Isolating triggered from induced events enables early and reliable identification of high-risk (Type B) mechanisms throughout the rock mass, a critical component in the development of effective and comprehensive seismic risk management plans. Data from Vale's Coleman Mine demonstrates how these parameters can be used to evaluate seismic source mechanisms, improve or independently corroborate traditional analysis results, and produce novel seismic source mechanism and risk maps.

Keywords: *mine seismicity, seismic analysis, seismic source mechanism, seismic risk*

1 Introduction

Unlike seismic source parameters and techniques originally developed for naturally occurring earthquakes, distance time (DT) parameters are designed to quantitatively describe seismic source mechanisms in mines. By explicitly considering discrete mine blasts, DT parameters facilitate probabilistic assessment of the underlying mechanisms driving dynamic rock mass failure processes in mines. Using automatically recorded blast-tagged events to generate a blasting record, these parameters are applied in real time to differentiate between stress fracturing and more complex failure processes.

1.1 Seismic source mechanisms in mines

Individual seismic events represent a snapshot of local conditions at that point in the larger rock mass failure process. Seismic source mechanism refers to the causative rock mass failure mode that generates a seismic event and can be used as a means of categorising mine seismicity. Figure 1 depicts source mechanisms within a hypothetical underground mining environment (Hudyma et al. 2003). Strong spatial clustering is observed in Figure 1a, which is a common phenomenon in mine seismicity (Kijko et al. 1993). In Figure 1b the seismic sources around typical underground workings are shown. It is around these seismic source mechanisms that seismicity clusters in Figure 1a.

Type A seismicity typically results from stress fracturing-related source mechanisms and is commonly observed within 100 m of mine blasting (Richardson & Jordan 2002). This type of failure is primarily controlled by the local state of stress and rock mass strength characteristics, and may occur in the presence or absence of pre-existing fractures (Woodward 2015). In Figure 1b, seismicity resulting from stress increase surrounding a small excavation within a high stress pillar is likely Type A — assuming the excavation was recently blasted and the local stress increase is proportional to the excavation geometry change.

---

[*] Corresponding author. Email address: laura@mineseismix.ca

Type B seismicity is often considered to be distant from mining-induced stress change but this is a convenient simplification. Throughout the course of mining, Type B source mechanisms in a rock mass are commonly located within the proximity of mining-induced stress change. Richardson & Jordan (2002) note that while Type A seismicity exhibits an upper seismic event magnitude bound near magnitude zero, exceptions have been documented. They observed that anomalously large, and presumably induced, seismic events appear to defy the simple classification scheme of Types A and B seismicity.
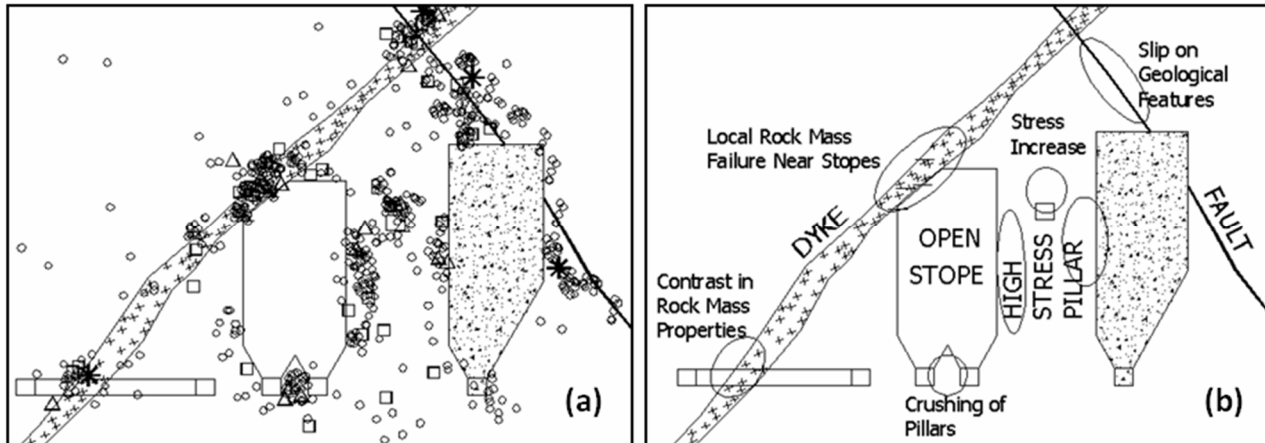

Figure 1   Variations in source mechanism within a mining environment are shown (Hudyma et al. 2003): (a) Hypothetical seismicity associated with a typical underground mine; (b) Seismic sources around typical underground mine workings

1.2   Complex seismic responses to mining

The fundamental characteristics of purely Type A and Type B seismic events in mines are constant but the characteristics of complex seismic responses depend on the relative proportions of Types A and B seismic events. Figure 2 depicts three time periods during the development of a mining drift. Within the mining environment shown is a single stationary dyke and a drift which is being developed over time. In (a) the drift is approaching the dyke, but the blast location is sufficiently far that the seismic response to mining is considered as an independent Type A response (outlined in blue) and an independent Type B response (outlined in red). As the drift is further developed and the blast location approaches the dyke, as shown in (b), the two independent responses become sufficiently close (in space) that they are joined into a single complex response (outlined in purple). The seismicity associated with the dyke is now occurring within the mining-induced stress change zone of the blast. As the mine drift continues to be developed and moves away from the dyke, as shown in (c), the Types A and B components of the complex response become sufficiently spaced that they are again perceived independently.
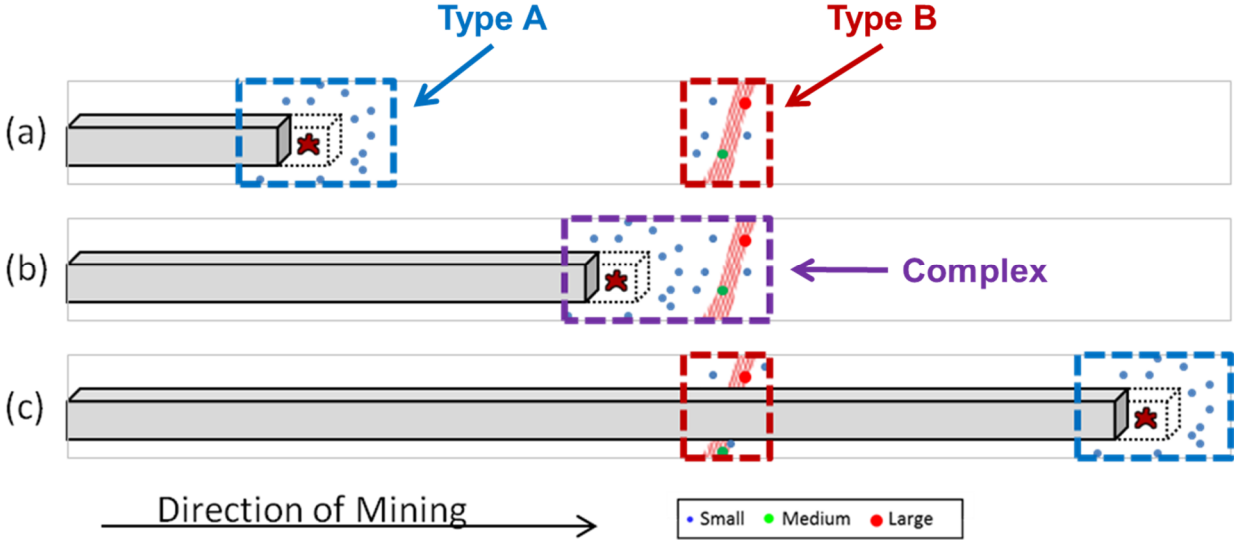
Figure 2   Examples of hypothetical Type A, Type B and complex seismic responses to typical development mining in an underground hard rock mining environment: (a) Types A and B responses are spatially isolated and considered separately; (b) Types A and B responses occur in the same place and are considered as a single complex response; (c) Mining progresses and Types A and B responses are once again spatially isolated and considered separately

1.3   Coleman mine

Vale's Coleman mine is a moderately deep underground operation with mining depths in the range of 1,500 to 1,800 m below surface. Variations of bulk open stoping and cut-and-fill mining are used across four main orebodies (153 OB, WOB, MOB and 170 OB) to extract copper, nickel and precious metals. Yao et al. (2014) and Landry & Reimer (2019) discuss specific challenges surrounding managing seismicity at Coleman mine. The hard rock mining environment is complex, with significant geological discontinues mapped across all orebodies as shown in Figure 3b. The significant differences in mining scale and rate, paired with the naturally complex environment and variations in seismic monitoring (see sensor locations in Figure 3a), make Coleman ideally suited for the testing of parameters designed to be reliable and robust indicators of seismic source mechanism.
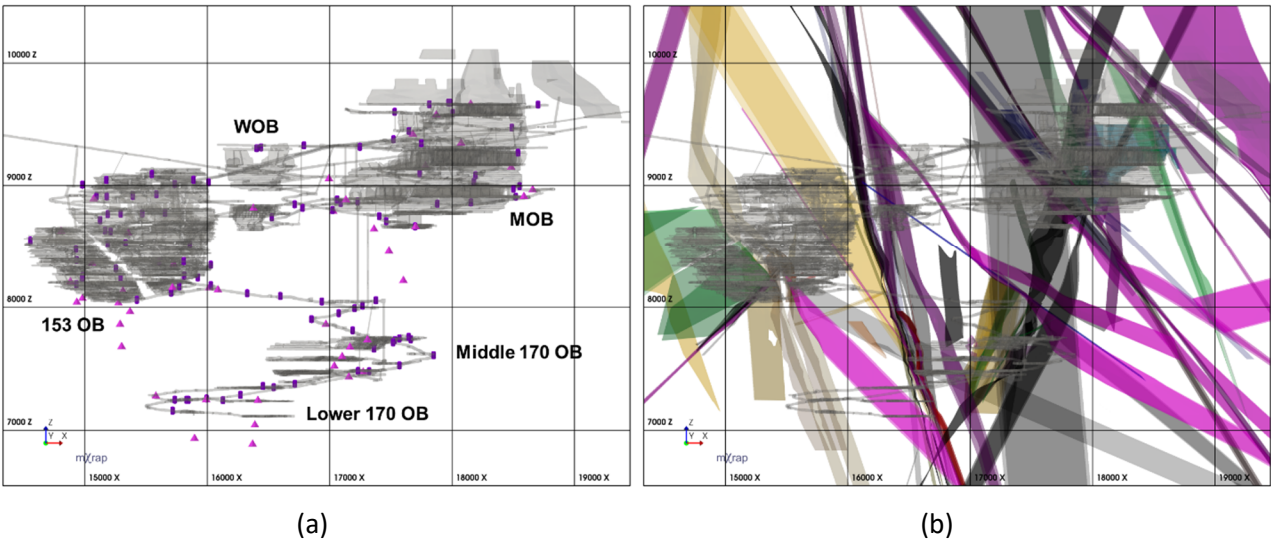

(a)

(b)

Figure 3   Cross-section of Coleman mine: (a) Seismic monitoring sensor locations; (b) Structural model of significant geological discontinuities

2   Methodology

DT parameters use seismic event time and location to quantitatively differentiate between Types A and B seismicity in mines. There is generally little to no error associated with seismic event time as times are recorded using a consistent timing source. Despite being the most reliable seismic source parameter, time is routinely considered only as a means of temporally isolating events from a larger dataset for more detailed analysis using other parameters. Event location error is routinely quantified for individual seismic events and is commonly less than 10 m for the majority of seismic events in Canadian mines (Brown & Hudyma 2018). By considering only time and location, error associated with DT parameters and analysis techniques is minimised and other parameters (such as seismic moment) may be used as an independent means of validating analysis results.

2.1   Calculating DT parameters

Figure 4 provides a high-level summary of all DT parameters. Brown (2020) outlines how base parameters are calculated using blast and seismic event times and locations. Considering mine-specific inputs, e.g. a maximum mining-induced stress change zone resulting from typical blasting, DT parameters are normalised to a unitless value between zero and one. A value of zero indicates a theoretically perfect Type A event that occurs in the same location and at the same time as a mine blast. A value of one indicates a theoretically perfect Type B event that occurs beyond the mining-induced stress change zone of the blast and at an independent time. Brown (2018) discusses the normalisation process in detail with examples from Agnico Eagle's LaRonde mine.

Summing all normalised parameters generates a unitless distance time index (DTI) ranging between zero and four. This serves as a single value indicator of how likely an event is of being Type A or Type B. Due to the unique combination of two independently calculated indices (blast index and cluster index, as shown in Figure 4), DTI has a built-in check and balance system that ensures increasingly reliable results as values approach the parameter distribution limits of zero and four for Type A and Type B, respectively.
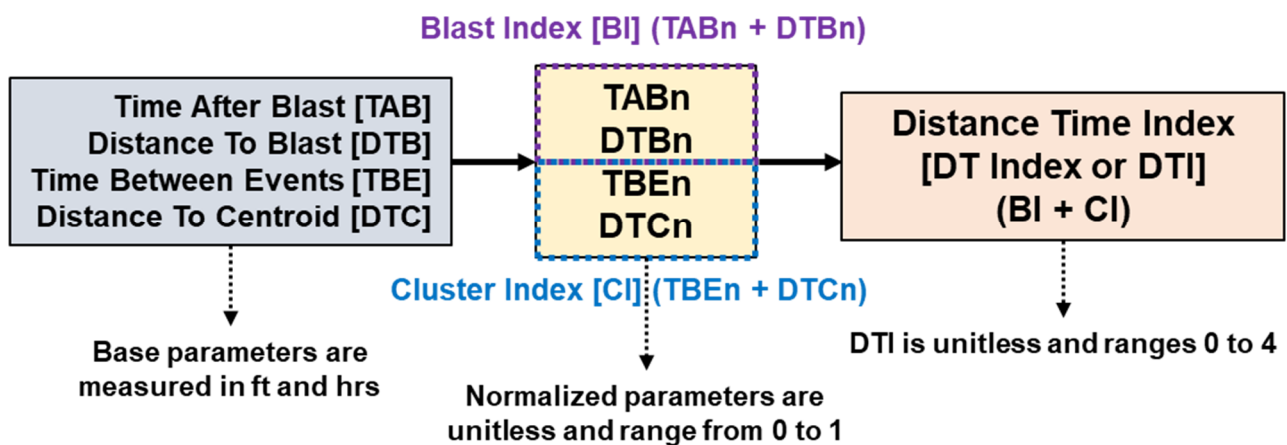

Figure 4   High-level summary of all distance time parameters

2.2   Blast record generation

A significant obstacle in the routine calculation of DT parameters is a reliable record of mine blast locations and times for both development and production mining. Fortunately, modern seismic monitoring and processing practices are often of sufficient quality to use blast-tagged seismic events (recorded by the seismic monitoring system) to automatically generate a reasonable blast record. This approach also ensures site staff do not have to update and maintain an independent blast record to calculate and assess DT parameters in real time.

As previously discussed, there is generally no error associated with event time for recorded ground motions, however, blast-tagged events must have reasonable location error residuals to be used reliably. Figure 5 depicts a 14-day trailing 90th percentile value of location residual for blast-tagged events at Coleman mine across five mining zones with varying monitoring coverage (Figure 3). Residuals for blasts are within reasonable limits as the 90th percentile is typically less than 9 m (approximately 30 ft, as shown on the Figure 5 y-axis) — particularly considering 2020 data forward.
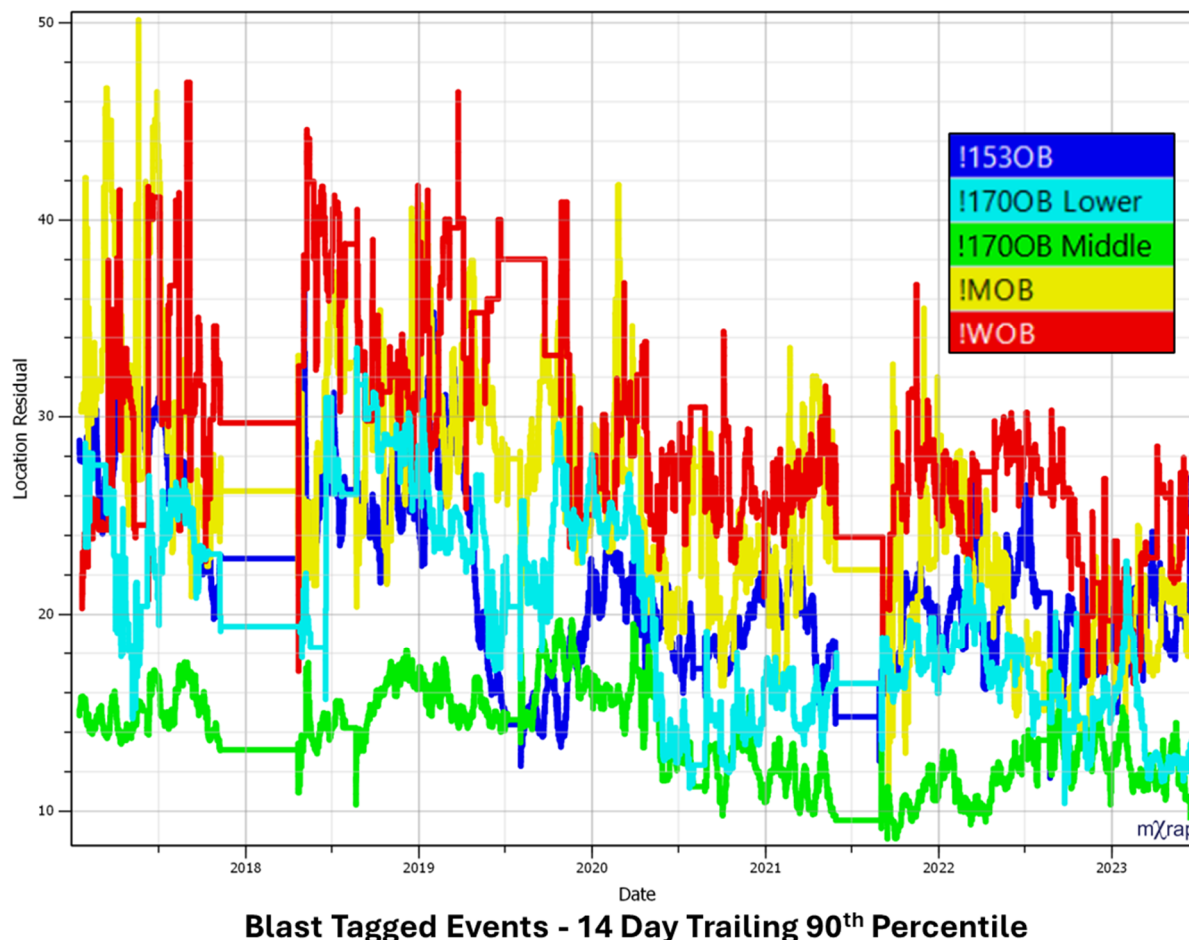

Blast Tagged Events - 14 Day Trailing 90ᵗʰ Percentile

Figure 5 Location residual (ft) time history chart showing a 14-day trailing of the 90th percentile for recorded blast-tagged events from 2017 to mid-2023 for all Coleman mining zones

2.3 Forming response clusters

For the calculation of cluster-related parameters (time between events and distance to centroid), a clustering methodology is required to group seismic events. Grid-based clustering is a widely applied analysis technique that minimises user input and bias (Wesseloo et al. 2014). Selecting a large grid that covers the entire mining zone with a sufficiently large grid spacing, in the range of 1.5 to 2.5 × sublevel spacing, ensures response clusters used in the calculation of DT parameters are appropriate for meaningful analysis. Seismic events are assigned to the closest grid point in space, and all events assigned to the same grid point in the same time period (bounded by consecutive blasting windows of typically 12 hours) form a cluster. Figure 6a depicts seismic events for the 4945L in the 153 OB from 2017 to 2024, coloured by cluster. Areas with multiple colours contain different clusters spread out across time. Cluster centroids (shown in Figure 6b) are densely concentrated in the most seismically active areas of the mining level for the time period considered.
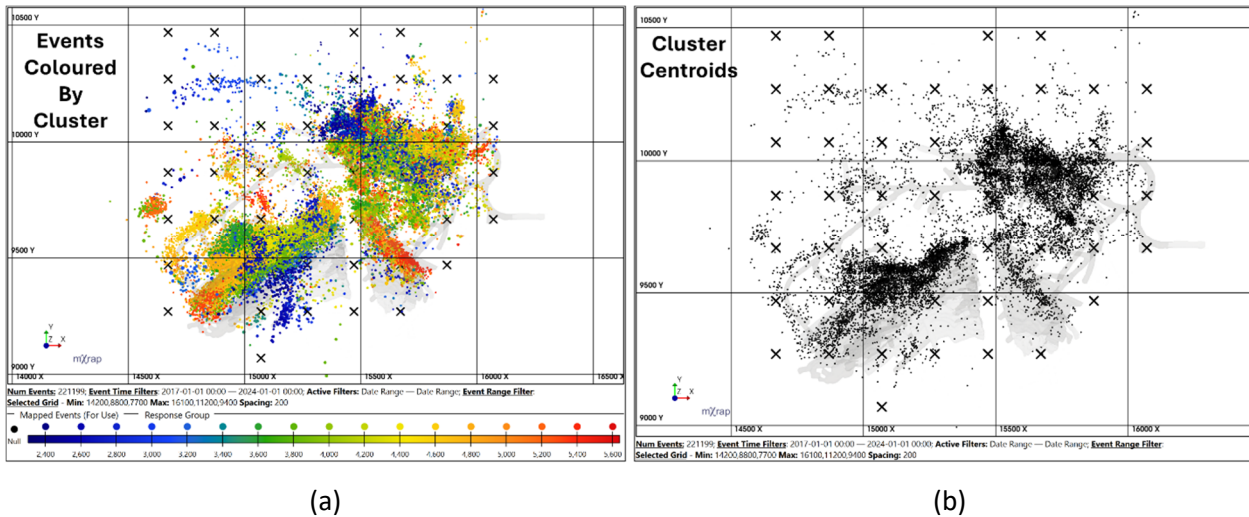
(a) (b)

Figure 6 4945L in the 153 OB at Coleman mine showing seismic events (2017–2024) and associated grid points (X symbols): (a) Events coloured by individual clusters over time; (b) Cluster centroid locations represented by black circles

3 Data and results

Seismicity can be effectively categorised into Type A and Type B events using DTI distributions, which provide clear and meaningful insight into the underlying rock mass failure mechanisms. Figure 7 depicts one week of seismic data from the 153 OB at Coleman mine with Types A and B seismic populations circled in blue and red, respectively. The Type A population surrounds recent mine blasting (indicated by red stars), while the adjacent Type B population occurs in a sill pillar with geological discontinuities. Where and when Type A and Type B seismicity overlap in space and time, complex seismicity is observed (circled in purple in Figure 7). The macroseismic events occurring in the complex population (shown as green and yellow spheres on the DTI distribution) are likely Type B as they exhibit DTI values greater than or equal to three. Colouring DTI distribution events by magnitude, which is not considered in the calculation of DT parameters, provides insight into seismic hazard and enables meaningful conclusions to be drawn surrounding seismic risk.
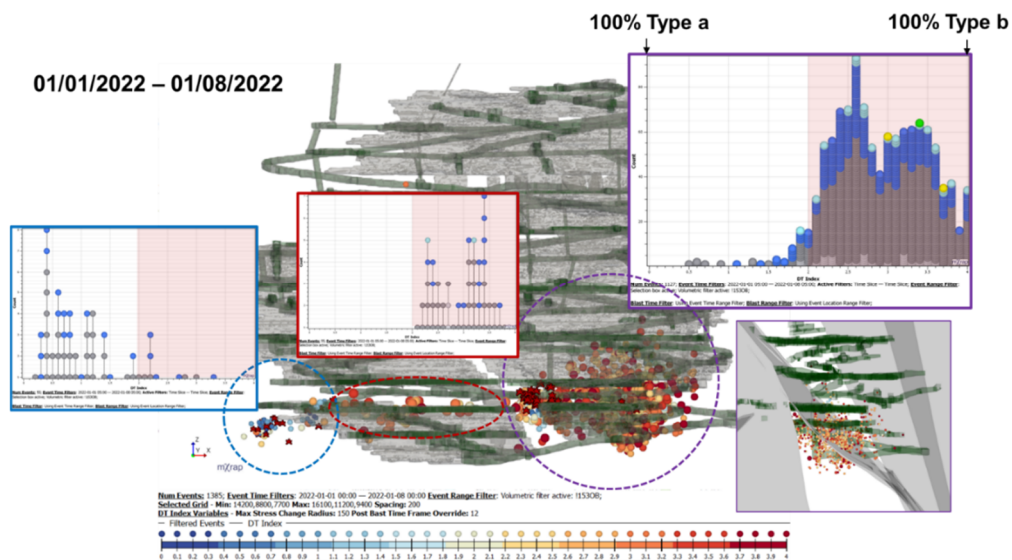

Figure 7 Example data from one week of mining (1–8 January 2022) in the 153 OB at Coleman mine. Events are coloured and sized according to DTI, and mine blasts (blast-tagged events) are shown as red stars. DTI non-cumulative distributions are provided for three different seismic populations, with events coloured by magnitude. The inset figure depicts the location of a geological discontinuity driving the rock mass failure (outlined in purple)

3.1 Bulk data validation

Calculating DT parameters for all seismic events at Coleman mine allows for bulk data to be evaluated and the methodology validated using site-specific knowledge and traditional seismic source parameters. Figure 8 depicts non-cumulative distributions of DTI for all 2023 seismic events in the MOB and Middle 170 OB. Events are coloured by magnitude, providing further insight into seismic hazard. The MOB is complex, with a high extraction ratio and several high seismic hazard geological structures that have been established as seismically active for many years (Figure 3). The vast majority of seismic activity in the MOB, both micro and macro, can be characterised as dominantly Type B – with DTI values greater than two and approaching four. The Middle 170 OB is a relatively new mining zone, with a lower extraction ratio and significant active mining undertaken throughout 2023. A different trend is observed in the Middle 170 OB data compared to the MOB. The Middle 170 OB microseismicity can be characterised as dominantly Type A while the majority of macro events (particularly M > 1) can be characterised as dominantly Type B; usually occurring as mining approaches known faults. These trends in DTI align with site experience gained through firsthand observations and general analysis results using traditional seismic parameters and techniques.
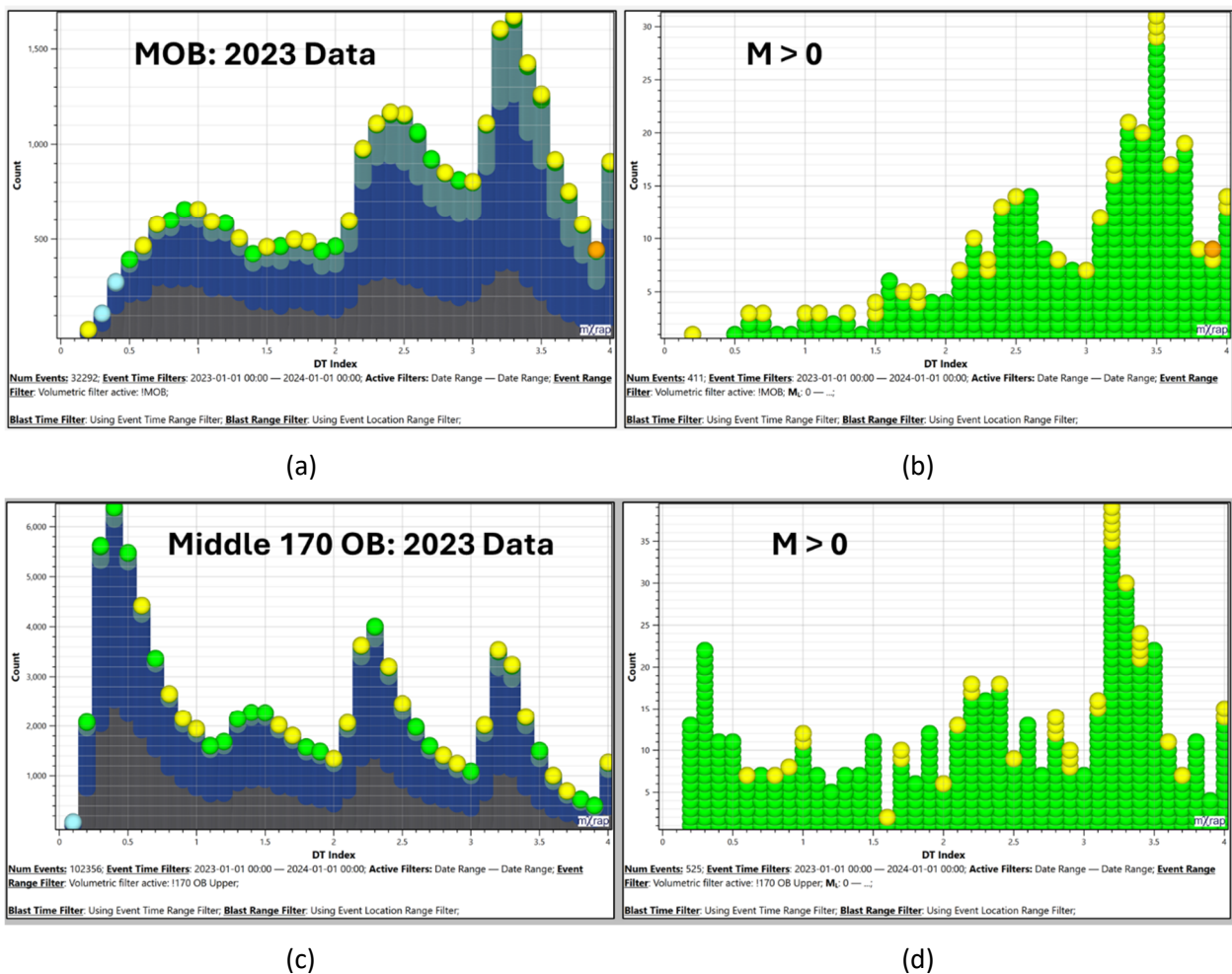

(a)

(b)

(c)

(d)

Figure 8   Non-cumulative distributions of DTI for 2023 seismic populations at Coleman mine: (a) Microseismicity occurring in the MOB coloured by magnitude; (b) Macroseismicity occurring in the MOB coloured by magnitude; (c) Microseismicity occurring in the Middle 170 OB, coloured by magnitude; (d) Macroseismicity occurring in the Middle 170 OB coloured by magnitude

Figure 9 depicts all data density isospheres (a), mapped blast locations (b), and high likelihood Type B (c) and Type A (d) density isospheres across all Coleman orebodies. The highest confidence Type A event concentrations (DTI < 0.1) directly correlate with blast locations throughout all mining zones and with all data for the 170 OB and WOB. The dominant seismic source mechanism for microseismicity in these zones is

known to be mining-induced stress change (Figure 8). In general, the Type A concentrations shown in Figure 9 are much larger and widely dispersed relative to the Type B concentrations, reflecting the dynamic nature of Type A source mechanisms (blasting) in mines. Highest confidence Type B event concentrations (DTI > 3.9) are fewer in number and highly localised throughout the mining environment. These areas typically surround known/mapped geological structures and in several cases directly follow structural wireframes across multiple mining levels and into the rock mass beyond the mined excavations.
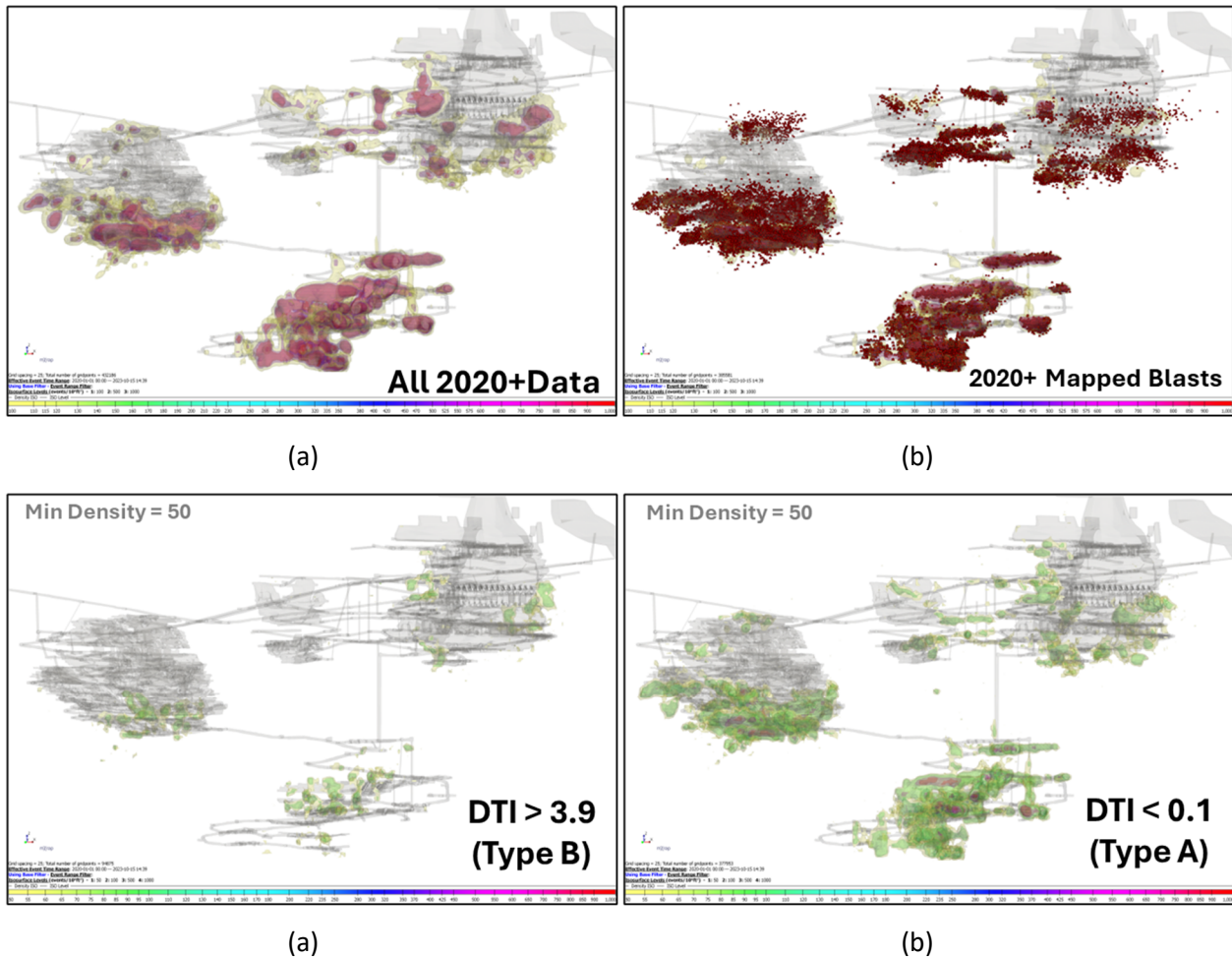

(a)   (b)

(a)   (b)

Figure 9   Coleman mine plots of density isospheres for data occurring from 2020 to October 2023: (a) Density isospheres considering all data; (b) All data density isospheres with mapped blast (blast-tagged event) locations shown as red stars; (c) Density isospheres considering only the highest confidence Type B events (DTI > 3.9); (d) Density isospheres considering only the highest confidence Type A events (DTI < 0.1)

3.2   Comparison with traditional parameters and analysis techniques

Large values of seismic moment and total radiated seismic energy correspond to large magnitude events and elevated seismic hazard. These independent seismic source parameters are often a primary consideration of traditional seismic analysis techniques but are completely independent of DT parameters (which only consider event time and location). Figure 10 depicts cumulative distributions of moment (a) and energy (b) using DTI value bins for all seismic events occurring in 2023 within the MOB. Each line represents an individual DT parameter bin of 0.5. For example, the dark blue line is comprised of all events $0 \leq DTI \leq 0.5$ and the dark red line is comprised of all events $3.5 \leq DTI \leq 4$. Clear trends of increasing moment and energy with increased DTI are evident, suggesting high DTI values may be associated with elevated seismic hazard, typical of Type B source mechanisms in mines.
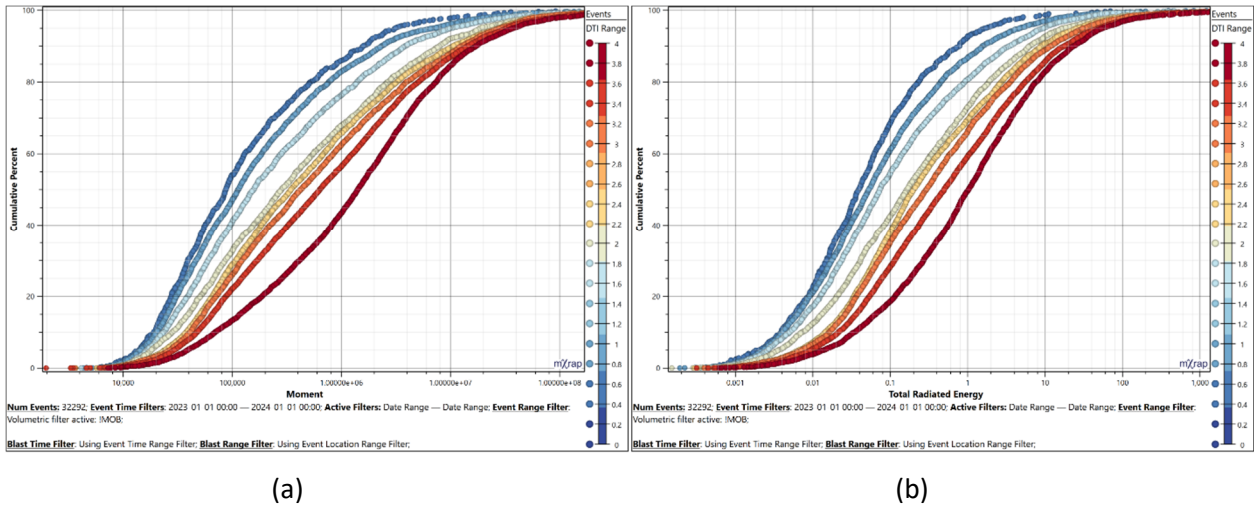
<center>(a)   (b)</center>

Figure 10 **Cumulative distributions of independent seismic source parameters not considered in the calculation of DT parameters. Each line represents an individual DT parameter bin of 0.5 for 2023 seismic data in the MOB: (a) Seismic moment; (b) Total radiated seismic energy**

Common traditional seismic analysis techniques used to gain insight into seismic source mechanisms in mines include frequency–magnitude relations, diurnal charts and S:P energy distributions (Hudyma 2008). Figure 11 depicts these analysis techniques alongside a non-cumulative DTI distribution for the most recent four years of data within approximately 9 m of a fault located within the MOB. This fault is known to be seismically active from physical observations underground, including a verified fault slip rockburst. DTI analysis (Figure 11a) clearly indicates a dominant Type B source mechanism, particularly for the macroseismic events. Comparatively, with a b-value of 1.35 (indicating a dominant stress fracturing mechanism), strong blasting influence evident in the diurnal distribution, and a relatively small proportion (35%) of events exhibiting S-wave energy to P-wave energy ratios (Es:Ep) greater than 10, the dominant Type B source mechanism of this dynamic rock mass failure process is not easily identified using traditional techniques (Figure 11b).
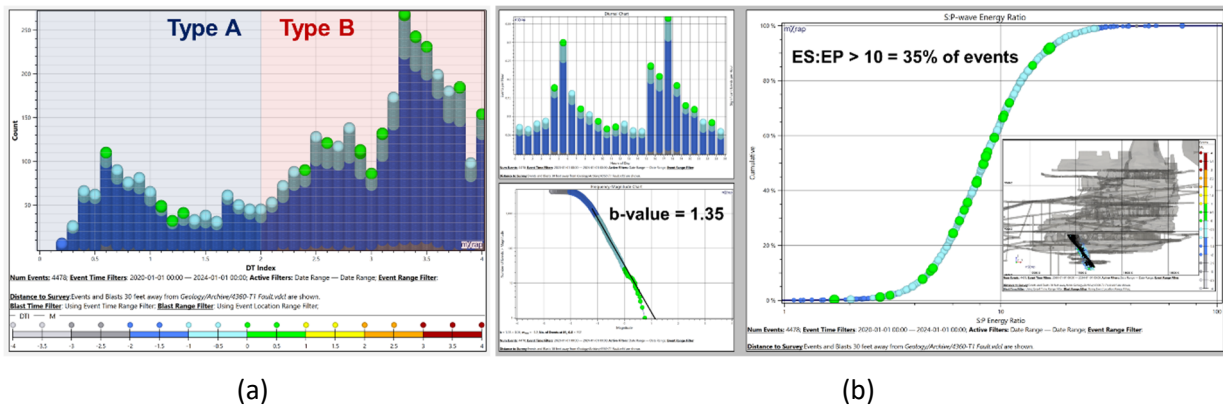

<center>(a)   (b)</center>

Figure 11 **Comparison of analysis techniques for seismic events within 9 m of 4360-T1 structure (in the MOB) occurring from 2020–2024; (a) DTI non-cumulative distribution with events coloured by magnitude; (b) Traditional seismic analysis techniques with events coloured by magnitude**

3.3 Spatial mapping

Spatial maps are a powerful tool that can be used to draw meaningful conclusions from large datasets relatively quickly. Figure 12 depicts the spatial mapping results for the 153 OB considering all seismic events occurring in 2023. Excavations are coloured according to the relative percent of high likelihood Type B events (DTI > 3), mapped from minodes using a search radius of 1.5 × sublevel spacing. The orange and red areas, highlighted by the red box in 12a, represent more than 15–20% of all high likelihood Type B activity (DTI > 3)

in the 153 OB. Use of a lower magnitude threshold ensures hot areas, exhibiting relatively high proportions of Type B activity, are also representative of elevated seismic hazard, as shown in Figure 12b.

DT parameter spatial maps highlight areas throughout a mine with ongoing dynamic rock mass failure consistently occurring spatially and temporally independent of discrete mine blasting activities – commonly referred to as active ground. Active ground is associated with elevated seismic risk as there is an increased and ongoing likelihood of workforce exposure. Plan views for the highlighted high Type B activity area in Figure 12 are shown with seismic events coloured by DTI (c) and mapped significant geological structures (d). The hotter coloured areas correlate well with seismically active structures. As shown in the inset images in (Figure 12d), only a single M > 1 event occurs in the hottest area during the 2023 time period considered. When all pre-2023 data is considered, however, there is a significant cluster of M > 1 events which further suggest the concentration of Type B activity is representative of elevated seismic hazard.
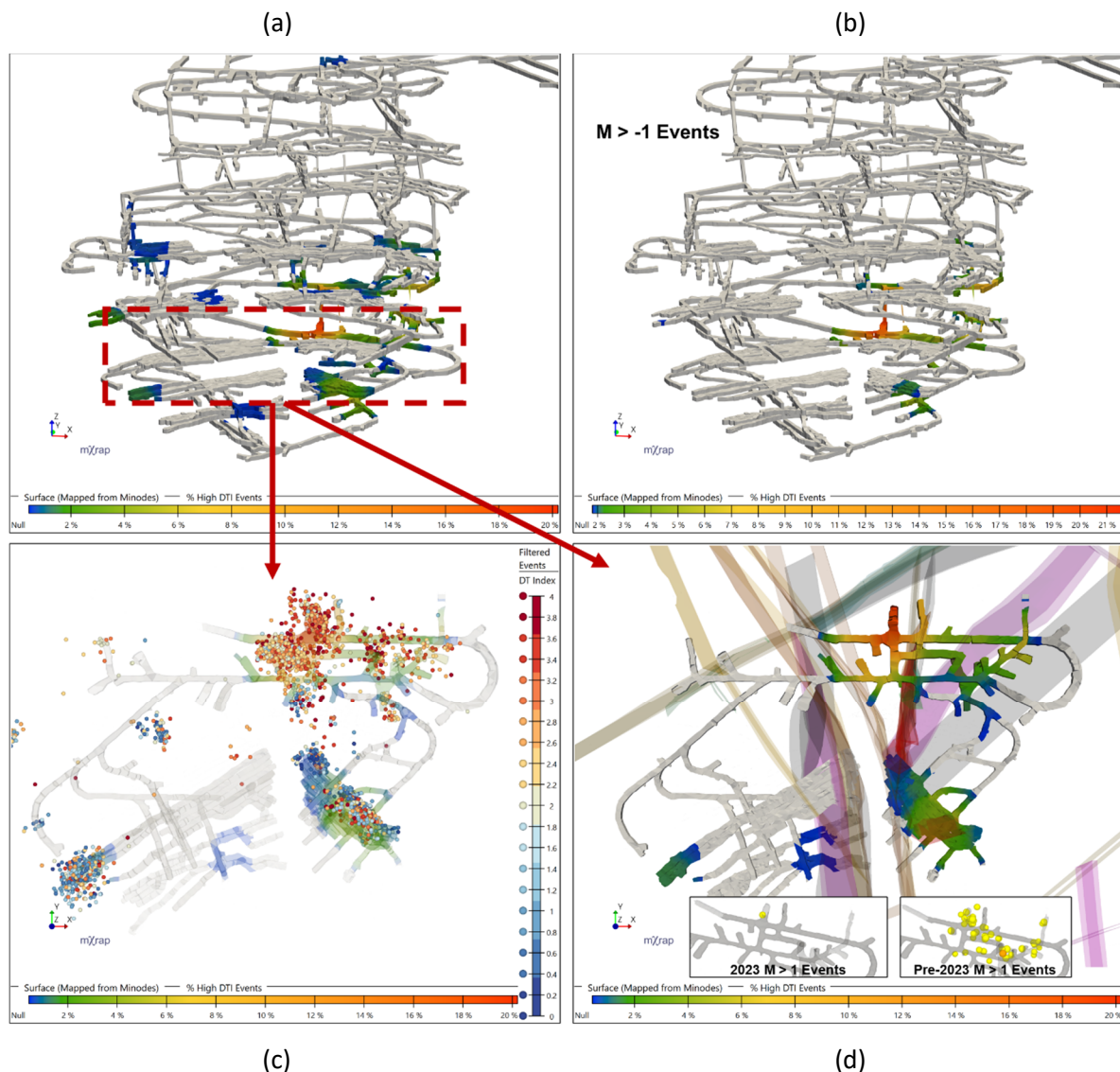

Figure 12 Spatial map for the 153 OB 2023 data. Excavations are coloured by the relative percent of high likelihood Type B events (DTI > 3) mapped from minodes using a search radius of 1.5 × sublevel spacing: (a) Map considering all magnitude events; (b) Map considering only M > –1 events; (c) Plan view of the mining level with the highest concentration of high likelihood Type B events (DTI > 3) showing events coloured by DTI; (d) Plan view of the mining level with the highest concentration of high likelihood Type B events (DTI > 3) showing mapped significant geological structures and insets of large magnitude events during the time period considered (left) and prior to the time period (right)

All mapped structures (wireframes) can be selected as a surface for spatial colouring using mXrap (Harris & Wesseloo 2015). Figure 13 depicts MOB structural wireframes (lunch room fault, diabase dykes, 3575 fault) coloured by the relative percent of high likelihood Type B events (DTI > 3) mapped from the closest grid point. Hot spots indicate relatively high Type B activity and correlate directly with structure intersections in proximity to significant (orebody scale) stress concentrations. This area contains several M > 2 events and is consequently representative of high seismic hazard. Using a specialised mXrap app, DT parameter maps can be quickly generated in real time to quantitatively highlight areas throughout a mine with significant Type B activity.
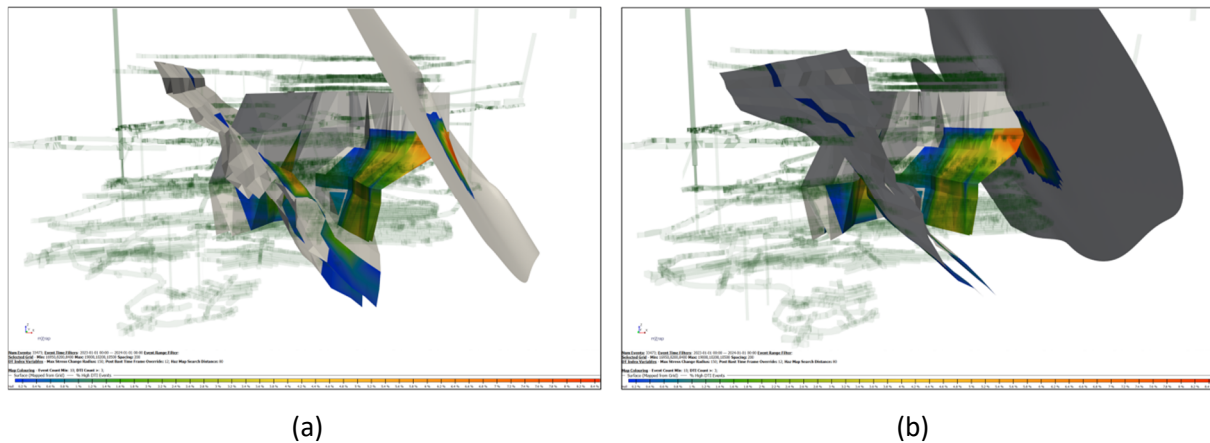

(a)   (b)

Figure 13 **Spatial map for the MOB 2023 data showing relative percent of high likelihood Type B events (DTI > 3) mapped from grid points onto geological structures (lunch room fault, diabase dykes, 3575 fault). Hot coloured areas (yellow – red) contain the highest proportion of Type B events in the MOB for 2023 and correlate directly with structure intersections. Two views, (a) and (b), are shown of the same map for perspective**

4   Discussion

Triggered dynamic rock mass failure is a significant hazard in deep and high stress mining operations. To systematically apply proactive seismic risk mitigation techniques, Type B source mechanisms must be identified early in the mining process — prior to the occurrence of large and potentially damaging seismic events. DT parameters are highly robust and directly applicable to poorly behaved seismic data (as defined by traditional standards, e.g. frequency–magnitude relations). By only considering seismic/blast-tagged event times and locations there is no dependence on triaxial sensors or concerns with sensor saturation. This makes them uniquely suited for source mechanism and seismic risk analysis in mining areas with reduced seismic monitoring coverage but significant worker exposure, such as active headings advancing the mining front.

5   Conclusion

Designed specifically for mine seismicity, DT parameters enable complex seismic responses to be probabilistically differentiated into Type A and Type B events. The use of normalised parameters ensures consistent and reliable interpretation across mining zones and between different mining operations. Nearly all traditional seismic analysis techniques can be complemented by DT analysis, which serves as an independent assessment of seismic source mechanism and as an indicator of seismic hazard and risk.

References

Brown, LG 2018, *Quantification of Seismic Responses to Mining Using Novel Seismic Response Parameters,* PhD thesis, Laurentian University, Sudbury.
Brown, LG 2020, 'Quantifying discrete seismic responses to mining', *Canadian Geotechnical Journal*, vol. 58, no. 7, pp. 1023–1035.
Brown, LG & Hudyma, MR 2018, 'Mining induced seismicity in Canada: a 2017 update', *Proceedings of the 52nd US Rock Mechanics/Geomechanics Symposium*, American Rock Mechanics Association, Alexandria.
Harris, PC & Wesseloo, J 2015, *mXrap*, version 5, computer software, Australian Centre for Geomechanics, The University of Western Australia, Perth, https://www.mxrap.com

Hudyma, MR 2008, *Analysis and Interpretation of Clusters of Seismic Events in Mines,* PhD thesis, The University of Western Australia, Perth.

Hudyma, MR, Heal, D & Mikula, P 2003, 'Seismic monitoring in mines - old technology - new applications', *Proceedings of the First Australasian Ground Control in Mining Conference*, Sydney.

Kijko, A, Funk, CW & Brink, AvZ 1993, 'Identification of anomalous patterns in time-dependent mine seismicity' in RP Young (ed.), *Proceedings of Rockbursts and Seismicity in Mines*, A.A. Balkema, Rotterdam, pp. 205–210.

Landry, D & Reimer, E 2019, 'Failure mechanisms and ground support observations at Coleman mine, Sudbury Basin', in J Hadjigeorgiou & M Hudyma (eds), *Ground Support 2019: Proceedings of the Ninth International Symposium on Ground Support in Mining and Underground Construction*, Australian Centre for Geomechanics, Perth, pp. 253–266, https://doi.org/10.36487/ACG_rep/1925_16_Landry

Richardson, E & Jordan, TH 2002, 'Seismicity in deep gold mines of South Africa: implications for tectonic earthquakes', *Bulletin of the Seismological Society of America*, vol. 92, pp. 1766–1782.

Wesseloo, J, Woodward, K & Pereira, J 2014, 'Grid-based analysis of seismic data', *The Journal of The Southern African Institute of Mining and Metallurgy*, vol. 114, pp. 815–822.

Woodward, KR 2015, *Identification and Delineation of Mining Induced Seismic Responses*, PhD thesis, The University of Western Australia, Perth.

Yao, M, Sampson-Forsythe, A & Punkkinen, AR 2014, 'Examples of ground support practice in challenging ground conditions at Vale's deep operations in Sudbury', in M Hudyma & Y Potvin (eds), *Deep Mining 2014: Proceedings of the Seventh International Conference on Deep and High Stress Mining*, Australian Centre for Geomechanics, Perth, pp. 291–304, https://doi.org/10.36487/ACG_rep/1410_19_Yao